Soft Matter

COMMUNICATION

View Article Online
View Journal | View Issue

Cite this: *Soft Matter*, 2024, **20**, 2881

Received 25th January 2024,
Accepted 1st March 2024

DOI: 10.1039/d4sm00122b

rsc.li/soft-matter-journal

Fluorescence-activated cell sorting (FACS) for purifying colloidal clusters†

Steven van Kesteren, ‡ Pascal Diethelm ‡ and Lucio Isa *

Colloidal particles are considered to be essential building blocks for creating innovative self-assembled and active materials, for which complexity beyond that of compositionally uniform particles is key. However, synthesizing complex, multi-material colloids remains a challenge, often resulting in heterogeneous populations that require post-synthesis purification. Leveraging advances brought forward in the purification of biological samples, here we apply fluorescence-activated cell sorting (FACS) to sort colloidal clusters synthesized through capillary assembly. Our results demonstrate the effectiveness of FACS in sorting clusters based on size, shape, and composition. Notably, we achieve a sorting purity of up to 97% for clusters composed of up to 9 particles, albeit observing a decline in purity with increasing cluster size. Additionally, dimers of different colloids can be purified to over 97%, while linear and triangular trimers can be separated with up to 88% purity. This work underscores the potential of FACS as a promising and little-used tool in colloidal science to support the development of increasingly more intricate particle-based building blocks.

1 Introduction

Crafting colloids with complex structures and non-uniform compositions has been a focal point for the soft matter community in recent decades.[1–3] Departing from uniform spherical particles and their corresponding isotropic properties and interactions unlocks the potential for colloidal units to self-propel[4–7] and self-assemble into intricate structures.[8–10] A favored method to obtain such complex colloidal building blocks is the assembly of spherical particles into well-defined clusters through diverse synthesis protocols such as emulsion templating, stimulated dewetting, colloidal fusion, or capillarity-assisted particle assembly.[7,8,11–14] However, these assembly processes seldom yield homogeneous populations of colloidal clusters, necessitating a post-synthesis purification step, especially for more intricate units. Various solutions have been proposed, each leveraging specific properties of the colloids. Among these methods, density-gradient centrifugation stands out as the most established,[14,15] effectively sorting clusters based on their mean density, and is ideally suited for assemblies comprising multiple materials with different densities. However, not all colloidal clusters can be separated by density differences, *e.g.*, clusters comprising particles made of the same materials but having different surface properties. Alternative approaches are often based on microfluidic separation, which has the capability to sort particles based on size, dielectric properties, magnetic susceptibility, or other parameters.[16–23] However, these microfluidic devices are often specialized tools that need to be specifically designed for each separation and have limited separation rates, thus making them difficult to integrate into colloid synthesis workflows.

Conversely, biologists have long been engaged in selecting and sorting cells and microorganisms out of heterogeneous populations. Among the different available developments, fluorescence-activated cell sorting (FACS) has emerged as a well-established method in various branches of biology, with readily available, user-friendly commercial devices.[24–27] In FACS, cells or microscopic entities are sequentially passed through a series of lasers and photodetectors that assess their scattering and fluorescence characteristics. Subsequently, the liquid stream containing these entities is subdivided into small droplets, each statistically containing no more than one entity. These droplets are then directed by electric fields into distinct containers according to the measured properties of the entity encapsulated within each droplet (schematically depicted in Fig. 1).[28] Despite its success and routine use in biology, the application of FACS has been starkly underexplored in colloidal science. Only recently, Mage *et al.* demonstrated an exciting study where they successfully sorted elliptical colloids with different aspect ratios based on their scattering characteristics.[29] Our work extends this exploration to fluorescence-based sorting of colloidal

Laboratory for Soft Materials and Interfaces, ETH Zurich, Vladmir-Prelog-Weg 1-5, Zurich, 8093, Switzerland. E-mail: lucio.isa@mat.ethz.ch

† Electronic supplementary information (ESI) available: Extended methods and additional experimental data. See DOI: https://doi.org/10.1039/d4sm00122b

‡ These authors contributed equally to this work.

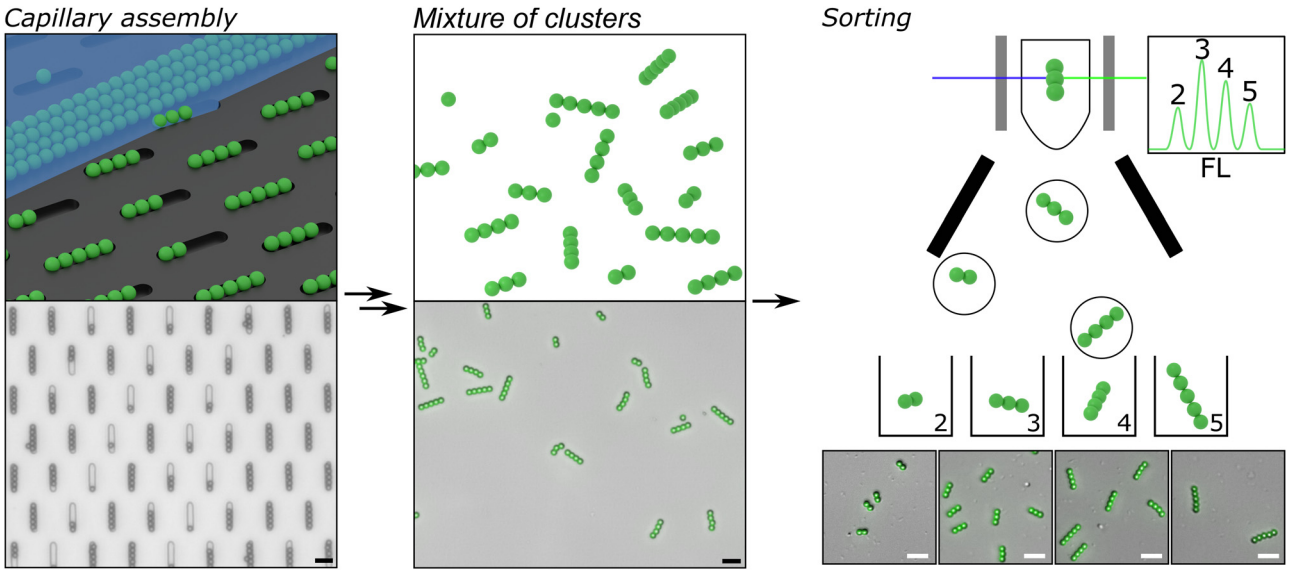

Fig. 1 Description of the fabrication and sorting of colloidal clusters: (left) top – schematics of capillarity-assisted particle assembly to create a distribution of colloidal clusters by purposefully underfilling the template. Bottom – bright-field microscopy image of a corresponding sample. After capillary assembly, the particles are sintered and harvested. (Middle) Schematic (top) and composite bright-field and fluorescence microscopy image (bottom) of the harvested clusters. (Right) Schematics showing the sorting of particle clusters with FACS based on their fluorescence intensity together with composite bright-field and fluorescence microscopy images of some sorted populations. Scale bars are 10 μm.

clusters, further exploring the potential of FACS in colloidal science by purifying samples of colloidal clusters based on size, composition, and shape.

To assess the applicability of FACS against a well-defined system of particles with clearly distinguishable characteristics, we use sequential capillarity-assisted particle assembly (sCAPA) to fabricate clusters of varying sizes and compositions. The sCAPA technique leverages the capillary forces of a receding droplet to meticulously deposit single or multiple colloids into microscopic wells with high precision and reproducibility.[12] This method proves particularly advantageous for our investigation, as it facilitates the generation of diverse discrete colloidal clusters from the same colloidal building blocks by adjusting the well geometry and deposition parameters.

In addition to the conventional sCAPA approach, which is optimized to achieve the highest uniformity of the assembled clusters, we deliberately employ sub-optimal deposition conditions to partially fill the wells, resulting in a heterogeneous mixture of colloidal clusters comprising different particle numbers. After deposition, the colloids are sintered together and harvested from the wells using a frozen water droplet.[12] The resulting colloidal clusters are then run through FACS, using both multiple fluorescence channels and forward and side scattering channels to discern and purify the various sub-populations. This experimental approach is outlined in Fig. 1 and discussed in detail in the Materials and methods.

2 Materials and methods

(1) Fabrication of the colloidal clusters by sCAPA

The green fluorescent (2.8 μ) and red fluorescent (2.5 μm) colloids used in this study were purchased from Microparticles GmbH. The colloidal clusters were fabricated using sCAPA, which has been described extensively in the literature.[12] In short, two distinct approaches were used to create the clusters for different experiments. Stochastic samples of long linear clusters between 1 and 9 particles were made in a single deposition step directed perpendicular to traps that can fit up to 5 or up to 9 colloids, respectively, using the following parameters: 6 mM sodium dodecyl sulfate (Sigma-Aldrich), 0.06% w/w Triton X-45 (Sigma-Aldrich), and 2 μm s^{-1} deposition speed. Conversely, dumbbells and three-particle clusters were made more purposefully (with high yield conditions) in multiple depositions using the following parameters: 2 mM sodium dodecyl sulfate (Sigma-Aldrich), 0.02% w/w Triton X-45 (Sigma-Aldrich), and 5 μm s^{-1} deposition speed. The traps for deposition were cast in PDMS (Sylgard 184) from masters fabricated in SU-8 through two-photon direct laser writing (Nanoscribe Photonic GT2).

After assembly, the filled traps were placed in an oven for 15 min at 110 °C to sinter the particles (see ESI,† Section 2 for details on the sintering temperature), and the sintered clusters were removed from the traps with a frozen water droplet following previously established procedures.[12] The droplets were then transferred and remelted in an Eppendorf tube.

(2) Quantification of sCAPA clusters by image analysis

The colloidal clusters obtained by sCAPA were quantified using fluorescence-microscopy images (Nikon, Eclipse Ti-2) and the MatLab script described in ESI,† Section 1.3. The script counts the various cluster sizes and distinguishes linear from non-linear clusters.

(3) Purification of colloidal clusters by FACS

FACS was performed using a BD-FACSAriaIII with a 70 μm nozzle, allowing for four sorting populations. Initially, the

individual fluorescent colloids and a small number of colloidal clusters are analyzed without sorting to determine the proper instrument setting and gate locations. For sorting, all colloidal clusters were preselected based on forward and side-scattering, excluding debris and larger aggregates. Sorting by size and particle composition was achieved using the fluorescence intensity of a 488/530 nm green channel and a 561/586 nm orange/red channel, and the shape was sorted using the forward-scattering width and height. The sorted samples were quantified using microscopy, and the populations were counted by hand (Nikon, Eclipse Ti-2). Detailed information on the gates can be found in the ESI,† Section 6.

3 Results

At first, we investigate sorting clusters containing up to five colloids. Image analysis of the initial suspension reveals a substantial presence of each sub-population, ranging from single colloids to pentamers (Fig. 2(a)). FACS data, represented in Fig. 2(c) as counts per green fluorescent intensity, exhibit distinct peaks corresponding to each sub-population, with the area under the peaks correlating with the population fractions determined through image analysis (see ESI,† Section 3 for the comparison between FACS and image analysis). Furthermore, the fluorescence scales linearly with cluster size. The FACS splits the initial suspension into four sub-populations: dimers, trimers, tetramers, and pentamers (2N to 5N). The compositions of the sorted populations are detailed in Fig. 2(d), highlighting a diminishing purity of the desired clusters with increasing size. For instance, the sorted population of dimers attains a purity of 96.8%, whereas the pentamers population achieves a purity of 76.4%.

We then repeat similar experiments, but extending the range to clusters containing up to nine particles in order to test the sorting limits. The distribution of these longer clusters, prepared in elongated wells, is shown in Fig. 2(b). As the used FACS machine allows sorting only up to four sub-populations

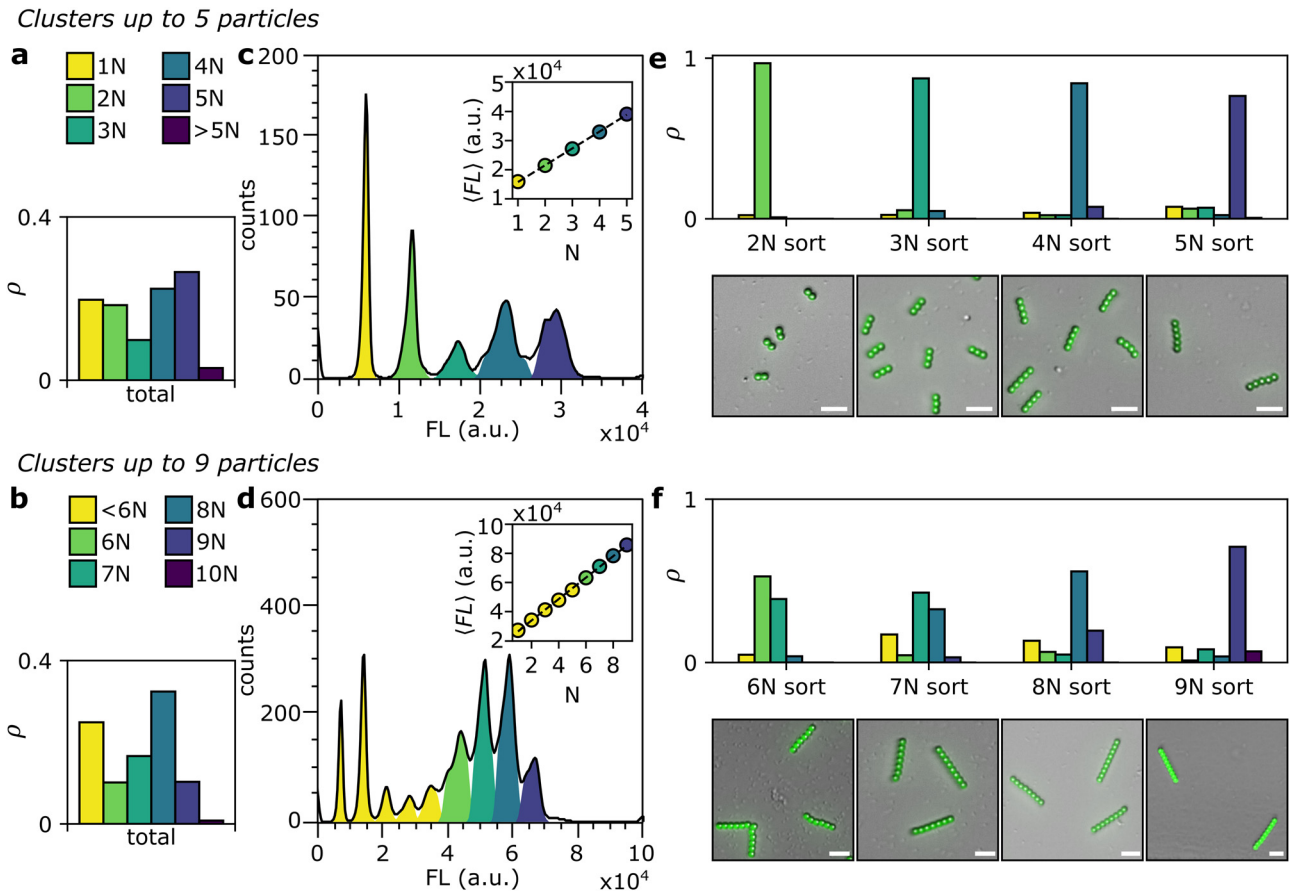

Fig. 2 Sorting mixtures of linear clusters: (a) and (b) distributions of clusters in the samples from analysis of microscopy data. (a) Corresponds to clusters made to be up to 5 particles (1367 clusters in total), and (b) corresponds to clusters made to be up to 9 particles (1219 clusters in total). (c), (d) Fluorescence histogram obtained through flow cytometry, the colored areas show the gated populations, and the solid black line is the histogram of the total sample. The inset shows the mean fluorescence as a function of cluster size (dots) with a linear fit (dashed line). (c) Corresponds to clusters up to 5 colloids (4510 counts in total), and (d) corresponds to clusters up to 9 colloids (17 710 counts in total). (e) and (f) Show the distribution of clusters after sorting obtained from analysis of microscopy data (top) and a representative composite fluorescent, bright-field micrograph (bottom). (e) Shows the sorting of clusters of 2 to 5 particles and (f) shows the sorting of clusters of 6 to 9 particles. At least 160 clusters are counted to obtain the distributions. Scale bars are 10 μm.

simultaneously, we focused on clusters ranging from six to nine colloids. Fig. 2(d) displays particle counts based on green fluorescence intensity, indicating distinct peaks for each cluster size, with fluorescence exhibiting linear scaling with cluster size. However, the increased overlap of populations, due to small property variations (size or fluorescence intensity) that accumulate over multiple particles, makes sorting of pure subpopulations more challenging, as depicted in Fig. 2(f). Although clusters are typically sorted within a limit of two colloids, a minimum single-size purity of 40.4% is achieved for the 7-mer case, and a purity of 69.9% is attained for the 9-mers, situated on the distribution's edge. For these overlapping populations, the exact placement and size of the gates likely control the combination of clusters. This gate placement could be improved through multiple iterations of sorting and analysis, as well as through automated data-driven algorithms.[30,31]

Besides single-material clusters, multi-material clusters can also be easily separated. Composite clusters of red and green colloids are used to demonstrate this application through the use of a second fluorescent channel. Specifically, red/green, red/red, and green/green dimers are made through sCAPA and subsequently mixed together (see ESI,† Section 4 for the details of the individual samples). The input population has three distinct sub-populations in similar fractions (Fig. 3(a)). The FACS data shows a clear distinction between the clusters (Fig. 3(b)). As a result, after sorting, the three populations all have a high purity $>97.8\%$.

Following the approach of Mage *et al.*,[29] we also explore the potential of using the scattering signals for sorting colloidal clusters of different shapes. Specifically, we prepare a mixture of linear and triangular trimers, made *via* sCAPA in rod or triangle-shaped wells, respectively, and subject it to sorting using FACS (see Fig. 4(a), and ESI,† Section 5 for the details of the individual samples). The fluorescence intensity was used to gate trimers, specifically. Additionally, the forward scattering width was also employed to distinguish between linear and triangular trimers (see Fig. 4(b)). Implementing these gating criteria, the sorted population exhibits a purity of 86.3% for the triangular trimers and 88.5% for the linear ones (Fig. 4(c)). These results underscore the robustness of utilizing scattering properties combined with fluorescence intensity to precisely sort colloidal clusters based on their distinct shapes.

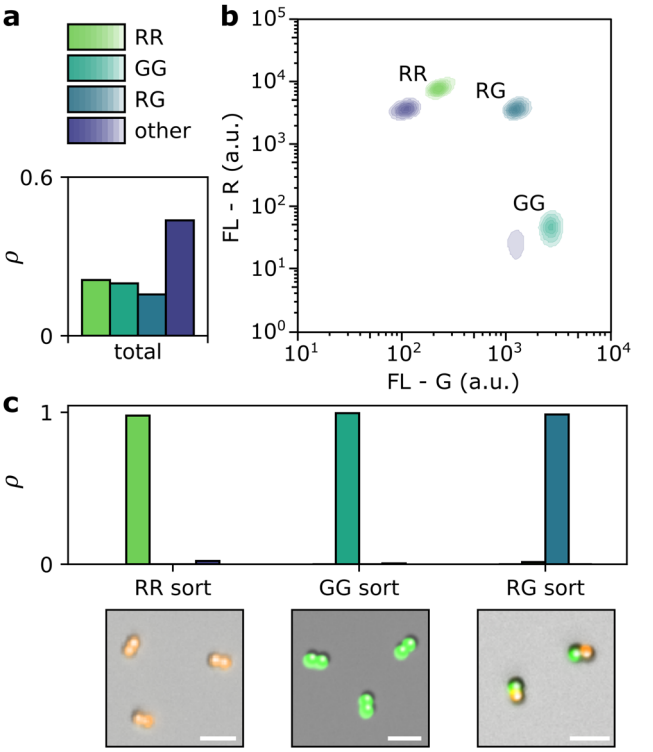

Fig. 3 Sorting clusters with mixed fluorescence: (a) cluster distribution in a mixed sample containing pure red fluorescent dimers (RR), pure green fluorescent dimers (GG), and dimers of one red and one green colloid (RG). The distribution is obtained from the analysis of microscopy data (1605 clusters in total). (b) Red and green fluorescence signals obtained from flow cytometry as density contours (10% per contour, 15 200 counts in total). The colors correspond to the gated populations. (c) Distribution of the RR, GG, and RG clusters after sorting, obtained from the analysis of microscopy data (top) and a representative composite fluorescence, bright-field micrograph (bottom). At least 370 clusters are counted to obtain the distributions. Scale bars are 10 μm.

4 Discussion and conclusions

In summary, our work showcases the potential of FACS as a robust and streamlined tool to purify polydisperse samples of complex colloids. In particular, we illustrate FACS's exceptional capability in efficiently sorting colloidal clusters based on size, composition, and shape, offering high promise in terms of specificity, versatility, and user-friendly operation.

However, while our findings present promising and consistent outcomes, it is crucial to address certain pitfalls and limitations associated with using FACS for purifying colloidal clusters. Foremost among these considerations is throughput, a critical factor in any purification process. In our specific experiments, we employed highly dilute samples containing approximately 10^5 clusters per milliliter, which were efficiently sorted within a few minutes. Modern FACS sorters can technically sort up to 70 000 particles per second.[28] However, the throughput of FACS may become a significant bottleneck for applications requiring sorting very dense colloidal suspensions, which can be orders of magnitude more concentrated. Notably, this limitation is not unique to FACS and is also present in most microfluidic approaches.

In general, the size range of FACS is defined by the dimensions of its nozzle and the sensitivity of its detection system, setting boundaries from approximately 100 μm to a few hundred nanometers for sortable clusters, depending on the particular setup and sorting requirements.[28] Additionally, we observed that, during FACS, substantial mechanical forces can be exerted onto the colloidal clusters, necessitating strong binding among colloids for the clusters to withstand the sorting process. Consequently, colloidal clusters held together by weak interactions are prone to breakage during sorting. Furthermore, our observations indicate a higher degree of fragmentation for larger

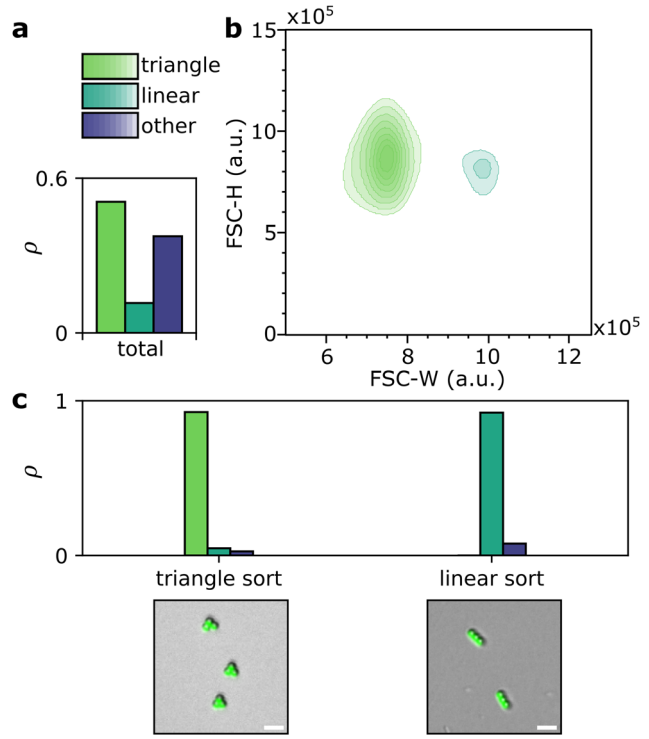

Fig. 4 Sorting mixtures of clusters with different shapes: (a) cluster distribution in a mixture containing clusters of three particles arranged in a line (linear) and in a triangle (triangle) obtained from the analysis of microscopy data (3394 clusters). (b) Forward scattering height (FSC-H) and forward scattering width (FSC-W) were obtained from flow cytometry as density contours (10% per contour, 6835 counts in total). The colors correspond to the gated populations. (c) Distribution of the linear and triangular clusters after sorting, as obtained from the analysis of microscopy data (top) and a representative composite fluorescence, bright-field micrograph (bottom). At least 160 clusters are counted to obtain the distributions. Scale bars are 10 μm.

clusters, as illustrated in Fig. 2(f) and further explored in ESI,† Section 2. This phenomenon suggests a potential limitation on the maximum cluster size that can be effectively sorted, irrespective of the FACS nozzle size. These considerations emphasize the importance of carefully assessing the specific requirements and characteristics of colloidal suspensions when contemplating using FACS for cluster purification.

Nonetheless, the increasing prevalence of FACS sorters in biological laboratories enhances accessibility for researchers across disciplines. Envisioning a future where FACS machines become common in colloid science labs, we foresee their use in achieving high-precision purification as a critical step to realize complex colloidal structures essential for advancing next-generation microswimmers,[32–34] self-assembly building blocks,[1,8] and colloidal-microorganism hybrids.[35,36]

Author contributions

Author contributions are defined based on the CRediT (Contributor Roles Taxonomy) and listed alphabetically. Conceptualization: L. I., S. v. K.; data curation: P. D., S. v. K.; formal analysis: P. D., S. v. K.; funding acquisition: L. I.; investigation: P. D., S. v. K.; methodology: L. I., S. v. K., P. D.; project administration: L. I.; software: P. D., S. v. K.; supervision: L. I.; validation: P. D., S. v. K.; visualization: L. I., P. D., S. v. K.; writing – original draft: L. I., P. D., S. v. K.; writing – review and editing: L. I., P. D, S. v. K.

Conflicts of interest

The authors declare no competing interest.

Acknowledgements

We thank the Flow Cytometry Core Facility from ETH Zürich, particularly Malgorzata Kisielow and Renan Antonialli, for their help with the flow cytometry experiments. This project has received funding from the European Research Council (ERC) under the European Unions Horizon 2020 Research and Innovation Program grant agreement no 101001514 and the Swiss National Science Foundation under the Postdoc.Mobility Grant no 217966.

Notes and references

1 T. Hueckel, G. M. Hocky and S. Sacanna, Total synthesis of colloidal matter, *Nat. Rev. Mater.*, 2021, **6**, 1053–1069.
2 A. B. Pawar and I. Kretzschmar, *Macromol. Rapid Commun.*, 2010, **31**, 150–168.
3 W. Li, H. Palis, R. Mérindol, J. Majimel, S. Ravaine and E. Duguet, *Chem. Soc. Rev.*, 2020, **49**, 1955–1976.
4 F. Ma, X. Yang, H. Zhao and N. Wu, *Phys. Rev. Lett.*, 2015, **115**, 208302.
5 S. Ni, E. Marini, I. Buttinoni, H. Wolf and L. Isa, *Soft Matter*, 2017, **13**, 4252–4259.
6 J. Palacci, S. Sacanna, A. P. Steinberg, D. J. Pine and P. M. Chaikin, *Science*, 2013, **339**, 936–940.
7 A. Aubret, Q. Martinet and J. Palacci, *Nat. Commun.*, 2021, **12**, 6398.
8 M. He, J. P. Gales, É. Ducrot, Z. Gong, G. R. Yi, S. Sacanna and D. J. Pine, *Nature*, 2020, **585**, 524–529.
9 S. N. Fejer, D. Chakrabarti and D. J. Wales, *Soft Matter*, 2011, **7**, 3553–3564.
10 É. Ducrot, M. He, G. R. Yi and D. J. Pine, *Nat. Mater.*, 2017, **16**, 652–657.
11 T. Hueckel and S. Sacanna, *ACS Nano*, 2018, **12**, 3533–3540.
12 S. Ni, J. Leemann, I. Buttinoni, L. Isa and H. Wolf, *Sci. Adv.*, 2016, **2**, 1–8.
13 M. Youssef, T. Hueckel, G. R. Yi and S. Sacanna, *Nat. Commun.*, 2016, **7**, 1–7.
14 D. J. Kraft, J. Groenewold and W. K. Kegel, *Soft Matter*, 2009, **5**, 3823–3826.
15 Z. Gong, T. Hueckel, G. R. Yi and S. Sacanna, *Nature*, 2017, **550**, 234–238.
16 S. Miltenyi, W. Müller, W. Weichel and A. Radbruch, *Cytometry*, 1990, **11**, 231–238.

17 N. Pamme, J. C. Eijkel and A. Manz, *J. Magn. Magn. Mater.*, 2006, **307**, 237–244.
18 H. Wei, B. H. Chueh, H. Wu, E. W. Hall, C. W. Li, R. Schirhagl, J. M. Lin and R. N. Zare, *Lab Chip*, 2011, **11**, 238–245.
19 P. Sajeesh and A. K. Sen, *Microfluid. Nanofluid.*, 2014, **17**, 1–52.
20 K. Zhao, M. Hu, C. van Baalen, L. Alvarez and L. Isa, *J. Colloid Interface Sci.*, 2023, **634**, 921–929.
21 T. Salafi, Y. Zhang and Y. Zhang, *Nano-Micro Lett.*, 2019, **11**, 3.
22 L. K. MÅnsson, T. D. Wild, F. Peng, S. H. Holm, J. O. Tegenfeldt and P. Schurtenberger, *Soft Matter*, 2019, **15**, 8512–8524.
23 W. Al-Faqheri, T. H. G. Thio, M. A. Qasaimeh, A. Dietzel, M. Madou and A. Al-Halhouli, *Microfluid. Nanofluid.*, 2017, **21**, 102.
24 S. F. Ibrahim and G. Van Den Engh, *Adv. Biochem. Eng./Biotechnol.*, 2007, **106**, 19–39.
25 S. Basu, H. M. Campbell, B. N. Dittel and A. Ray, *J. Visualized Exp.*, 2010, 3–6.
26 R. J. Bleichrodt and N. D. Read, *Fungal Biol. Rev.*, 2019, **33**, 1–15.
27 I. Antoniadi, V. Skalický, G. Sun, W. Ma, D. W. Galbraith, O. Novák and K. Ljung, *Cytometry, Part A*, 2022, **101**, 725–736.
28 BD Biosciences European Customer Support BD FACSAria™ III User's Guide, 23-11654-01, 2012, vol. 1, pp. 273–276.
29 P. L. Mage, A. T. Csordas, T. Brown, D. Klinger, M. Eisenstein, S. Mitragotri, C. Hawker and H. T. Soh, *Nat. Mater.*, 2019, **18**, 82–89.
30 B. Anchang, M. T. Do, X. Zhao and S. K. Plevritis, *PLoS Comput. Biol.*, 2014, **10**, 1–14.
31 J. S. Yu, D. A. Pertusi, A. V. Adeniran, K. E. Tyo and J. Wren, *Bioinformatics*, 2017, **33**, 909–916.
32 L. Alvarez, M. A. Fernandez-Rodriguez, A. Alegria, S. Arrese-Igor, K. Zhao, M. Kröger and L. Isa, *Nat. Commun.*, 2021, **12**, 4762.
33 S. van Kesteren, L. Alvarez, S. Arrese-Igor, A. Alegria and L. Isa, *Proc. Natl. Acad. Sci. U. S. A.*, 2023, **120**, 1–9.
34 T. Y. Huang, H. Gu and B. J. Nelson, *Annu. Rev.*, 2022, **5**, 279–310, DOI: **10.1146/annurev-control-042920-013322**.
35 L. Schwarz, M. Medina-Sánchez, O. G. Schmidt and M. M.-S. Anchez, *Appl. Phys. Rev.*, 2017, **4**, 31301.
36 G. Z. Lum, A. Klingner, J. Simmchen, J. Bastos-Arrieta, A. Revilla-Guarinos and W. E. Uspal, *Front. Robot. AI.*, 2018, **1**, 97.